ELSEVIER

Journal of Power Sources 81–82 (1999) 44–48

JOURNAL OF POWER SOURCES

www.elsevier.com/locate/jpowsour

Defect chemical aspects of lithium-ion battery cathodes

J. Schoonman [a,*], H.L. Tuller [b], E.M. Kelder [a]

[a] *Delft Interfaculty Research Center, Renewable Energy, Laboratory for Inorganic Chemistry, Delft University of Technology, Julianalaan 136, 2628 BL Delft, Netherlands*

[b] *Department of Materials Science and Engineering, Massachusetts Institute of Technology, Cambridge, MA 02139, USA*

Abstract

Structural and defect structural aspects of lithiated layer-structured transition-metal oxides with the α-$NaFeO_2$ structure will be discussed in relation to stability and electrical behaviour. Emphasis will be put on anti-site disorder in $LiNiO_2$. The defect structures of lithiated spinel-structured $LiMn_2O_4$ are quite dependent on the Li/Mn ratio and the dopants. Even defect clusters have been proposed to occur in non-stoichiometric $LiMn_2O_4$. It will be shown that important information on the defect structures can be obtained from magnetic and electron spin resonance (ESR) experiments on lithium-deficient $Li_{1-x}Mn_2O_4$ and lithium-excess spinel $Li_{1+d}Mn_{2-d}O_4$. The number of unpaired electrons provides information on the distribution of electrons over the t_{2g} and e_g orbitals. The Curie temperature provides information on cation–cation and cation–anion–cation interactions.

Keywords: Cathode materials; Defect chemistry; Lithium ion battery; Magnetic susceptibility; Electron spin resonance

1. Introduction

The electrochemical and structural properties of nominally pure and doped lithium–nickel, lithium–cobalt, and lithium–manganese oxides have attracted widespread attention in the recent literature [1]. These materials are of interest as positive electrode for rechargeable lithium-ion batteries. Moly Energy utilises $LiNiO_2$ [2], Sony Energytec $LiCoO_2$ [3], while Bellcore applies $LiMn_2O_4$ [4] in lithium- and lithium-ion batteries.

These types of batteries are being developed for a variety of applications, ranging from solid-state microbatteries deposited on chip carriers to provide memory back-up power, as power supply in sensors, biomedical implantable devices and portable electronics, to high-power density batteries for electric vehicles and decentralized storage of, for instance, photovoltaic electricity for large-scale introduction of renewable energy.

In the mixed ionic-electronic conducting cathode materials the diffusion of the lithium ions controls to a large extent the electrical properties. Because for practical applications polycrystalline materials are used, relations between structure, defect structure, microstructure and mass and charge transport properties are to be considered in optimizing the electrical properties of these cathode materials.

The lithiated layer-structured-transition metal oxides adopt the same α-$NaFeO_2$ structure. Yet their phase stability and defect structures differ. A phase transition to an electrochemical inactive structure is only partly reversible in $LiNiO_2$, but reversible in $LiCoO_2$. More lithium can be extracted from $LiCoO_2$ than from $LiNiO_2$ before structural degradation occurs. In addition, substantial anti-site defect disorder occurs in $LiNiO_2$. Doping has been studied to stabilize the structure of $LiNiO_2$ and to improve its electrical behaviour. The defect structures of, in particular, $LiNiO_2$ will be discussed.

In order to improve both the practical capacity as well as the stability of spinel-structured $LiMn_2O_4$, a variety of dopant ions have been studied, among which Li, leading to $Li_{1+d}Mn_{2-d}O_4$ with $0 < d < 1/3$ has proven to be successful. Addition of extra lithium increases the oxidation state of manganese and as a consequence to a reduction of the theoretical capacity. The defect structures of the as-synthesized materials are different if the extra lithium ions replace the regular Mn(III) 16d sites, or accommodate the 16c sites.

In the case of Li-extraction, vacancies are formed on 8a sites in the lithium-ion sublattice. Models based on the formation of a partially inverse spinel structure have been

* Corresponding author

0378-7753/99/$ - see front matter
PII: S0378-7753(99)00128-7

proposed [5], while defect clusters, comprising oxygen ion vacancies and manganese ions with an effective negative charge, have been described in the literature [6,7]. Extrinsic and intrinsic defect structures of nominally pure and doped $LiMn_2O_4$ will be discussed.

As the defect structures influence both the ionic and electronic properties of the spinel material, magnetic susceptibility and electron spin resonance (ESR) experiments were performed on the lithium-deficient and lithium-excess spinel materials. The existence of high-spin and low-spin states of Mn(III) ion was established, while the ESR results indicated the electron distributions over the t_{2g} and e_g orbitals. It will be shown that by using the electronic structure actual defect structures can be derived.

2. Structural and defect-chemical aspects

2.1. $LiCoO_2$ and $LiNiO_2$ [8–12]

These compounds adopt a layer structure with prototype α-$NaFeO_2$ and space group *R3m* with a hexagonal setting comprising basically the lithium ions in the 3b sites, the transition metal ions in the 3a sites, and the oxide ions in the 6c sites. Removal of the lithium ions tends to de-stabilize the crystal structure due to the increasing repulsion between the bare oxide layers that face each other. An advantage of the $LiCoO_2$ over $LiNiO_2$ is that a significant higher number of lithium ions can be removed upon charging before the structure becomes unstable with respect to displacement of the transition metal oxide layers.

At elevated temperatures both $LiNiO_2$ and $LiCoO_2$ undergo phase transitions from the hexagonal to a cubic phase. The hexagonal phase is electrochemically active, the cubic phase not. The phase transition for $LiCoO_2$ is reversible, whereas the phase transition for $LiNiO_2$ is only partially reversible and slow. As a consequence, equimolar $LiNiO_2$ is more difficult to prepare that $LiCoO_2$ and the pristine phase is usually denoted as $Li_{1-y}Ni_{1+y}O_2$ or $[Li_{1-y}Ni_y]_{3b}[Ni]_{3a}O_2$ with x being about 0.005. In case of equimolar $LiNiO_2$ a strong temperature dependency of cation mixing in $LiNiO_2$ has been reported [12]. They found about 13% of the lithium ions to be in 3a sites and a similar amount of Ni(III) in 3b sites at 700°C. These 3a Li^+ ions will not contribute to the capacity, and are therefore lost. Moreover, during extraction of Li^+ ions, Ni(III) ions tend to redistribute in order to stabilize the material, i.e., 3a Ni(III) ions move to 3b sites. Upon firing above 720°C in air, the electrochemically active hexagonal phase transforms into an inactive cubic phase. It has also been found that up to 615°C the impedance spectra are frequency invariant, indicating a predominantly electronic conductivity [11].

Stabilization can be reached also by addition of extra Ni ions, which occupy the 3b Li sites: $Li_{1-y}Ni_{1+y}O_2$ or $[(Li^x_{Li})_{1-y}(Ni^{\cdot}_{Li})_y]_{3b}[(Ni^x_{Ni})_{1-y}(Ni'_{Ni})_y]_{3a}O_2$. Charge compensation can in principle be established by interstitial oxygen (O''_i), oxygen vacancies ($V^{\cdot\cdot}_O$), or electrons ($2e'$). The crystal structure is not suitable for O''_i, but $V^{\cdot\cdot}_O$ (1) and e' (2) may be present. In defect notation the compositions read

1. $(Li^x_{Li})_{1-y}(V'_{Li})_{2y}(Ni^x_{Ni})_{1+y}(O^x_O)_2(V^{\cdot\cdot}_O)_{2y}(e')_{2y}$ with electroneutrality condition: $[V'_{Li}] + [e'] = 2[V^{\cdot\cdot}_O]$
2. $(Li^x_{Li})_{1-y}(Ni^{\cdot\cdot}_{Li})_y(Ni^x_{Ni})(O^x_O)(e')_{2y} \leftrightharpoons (Li^x_{Li})_{1-y}(Ni^{\cdot}_{Li})_y(Ni^x_{Ni})_{1-y}(Ni'_{Ni})_y(O^x_O)_2$ reflecting electron trapping at Ni(III) in a Li 3b site and at Ni(III) in a 3a site.

It appears that even a small amount of excess nickel has a dramatic influence on the capacity, since it influence strongly the nickel oxidation state. Further stabilization has been studied by adding dopants, Li(Ni,M)O_2, with M = Al [13], Ga, Mn, and Co. Anion doping has also been explored using fluorine, i.e., $Li_{1+y}Ni_{1-y}O_{2-z}F_z$ [14]. In this case, the fluorine opens up the possibility to compensate for the changed oxidation state upon Ni addition, i.e., $z = 2y$.

2.1.1. Extracted forms of $Li_{1-x}NiO_2$

$Li_{1-x}NiO_2$ adapts to lithium removal by phase changes, i.e., hexagonal ($x < 0.25$), monoclinic ($0.25 < x < 0.5$), and cubic ($x > 0.7$) structure. For $x > 0.7$, a disordered rock–salt structure results from random nickel and lithium ion mixing.

Both $Li_{1-x}NiO_2$ and $Li_{1-x}CoO_2$ exhibit a weight loss which is attributed to loss of oxygen and shall lead to deviations from stoichiometry. The thermal stability of $Li_{1-x}NiO_2$ is smaller than that of $Li_{1-x}CoO_2$, because Ni^{3+} is more readily reduced than Co^{3+}.

2.1.2. O_2 evolution of $LiNiO_2$

The extracted form $Li_{1-x}NiO_2$ looses oxygen above 190°C if $x > 0.1$. This can be written in defect notation as follows:

$$O^x_o \leftrightharpoons 1/2O_{2(g)} + V^{\cdot\cdot}_O + 2e' \qquad K_1$$

$$Ni^x_{Ni} + e' \leftrightharpoons Ni'_{Ni} \qquad K_2$$

$$O^x_o + 2Ni^x_{Ni} \leftrightharpoons 1/2O_{2(g)} + V^{\cdot\cdot}_O + 2Ni'_{Ni} \qquad K_3$$

$$K_1 = K_2^{-2}K_3$$

The electroneutrality condition reads $2[V^{\cdot\cdot}_O] = [e'] + [Ni'_{Ni}]$ and two regimes can be distinguished, i.e.:

Regime I: $2[V^{\cdot\cdot}_O] = [e'] = 2K_1^{1/3}p_{O_2}^{-1/6}$
Regime II: $2[V^{\cdot\cdot}_O] = [Ni'_{Ni}] = 2K_3^{1/3}p_{O_2}^{-1/6}$

Based on the predominant defects present in either regime it is apparent that the electrical properties in regime I will be governed by electronic conductivity, and in regime II by ionic conductivity. Hence, no frequency dispersion will be observed in impedance spectroscopical measurements, if the material is with regard to its composition in regime I.

At even higher temperatures, thermal decomposition takes place, i.e.,

$$Li_{1-x}NiO_2 \rightarrow (2-x)Li_{(\{1-x\}/\{2-x\})}Ni_{(1/\{2-x\})}O + 1/2\,xO_{2(g)}$$

with $Li_{(\{1-x\}/\{2-x\})}Ni_{(1/\{2-x\})}O$ having the rock–salt structure $Li_{1-a}Ni_aO$ [5].

2.1.3. Anti-site disorder: $Li_{1-y}Ni_{1+y}O_2$

$$O_o^x \leftrightharpoons 1/2O_{2(g)} + V_O^{\cdot\cdot} + 2e' \qquad K_1$$

$$Ni_{Li}^{\cdot\cdot} + e' \leftrightharpoons Ni_{Li}^{\cdot} \qquad K_4$$

$$O_o^x + 2Ni_{Li}^{\cdot\cdot} \leftrightharpoons 1/2O_{2(g)} + V_O^{\cdot\cdot} + 2Ni_{Li}^{\cdot} \qquad K_5$$

$$K_4 = K_1^{-1/2}K_5^{-1/2}$$

The electroneutrality condition is $2[V_O^{\cdot\cdot}] + 2[Ni_{Li}^{\cdot\cdot}] + [Ni_{Li}^{\cdot}] = [e']$, and four regimes can be distinguished, i.e.:

Regime I: $2[V_O^{\cdot\cdot}] + 2[Ni_{Li}^{\cdot}] = [e']$
Regime II: $2[Ni_{Li}^{\cdot\cdot}] = [e'](\neq f(p_{O_2}))$
Regime III: $2[V_O^{\cdot\cdot}] + [Ni_{Li}^{\cdot}] = [e']$
Regime IV: $[Ni_{Li}^{\cdot}] = [e'](\neq f(p_{O_2}))$

The defect concentrations in regimes I and III are a function of the oxygen partial pressure. The defect concentrations in regimes II and IV are not dependent on the oxygen pressure.

2.1.4. Extracted forms of $Li_{1-y-x}Ni_{1+y}O_2$

Delmas et al. [8] describe the changes in oxidation state of the Ni ions during the first extraction cycle. Their starting composition was $Li_{1-x}Ni_{1+x}O_2$. In defect notation the structure can be written (with $LiNiO_2$ as the reference material and Li^+ stands for a lithium ion donated or accepted from the electrolyte) as:

extraction: step 1: $Li_{Li}^x + Ni'_{Ni} \rightarrow V'_{Li} + Ni_{Ni}^x + Li^+ + e'$
step 2: $Li_{Li}^x + Ni_{Ni}^x \rightarrow V'_{Li} + Ni_{Ni}^{\cdot} + Li^+ + e'$
step 3: $Li_{Li}^x + Ni_{Li}^{\cdot} \rightarrow V'_{Li} + Ni_{Li}^{\cdot\cdot} + Li^+ + e'$
insertion: step -2: $V'_{Li} + Ni_{Ni}^{\cdot} + Li^+ + e' \rightarrow Li_{Li}^x + Ni_{Ni}$

Hence, steps 1 and 3 of the extraction process are not reversible, and therefore lead to capacity reduction. Furthermore, the oxidation of the Ni(II) ions induces a local disruption of the interslab MO_2 space making the insertion step more difficult.

2.2. $LiMn_2O_4$ [15–19]

This compound adopts the spinel structure. The prototype of this structure is $MgAl_2O_4$ having a space group *Fd3m* with a cubic setting. The lithium ions basically occupy the tetrahedral 8a sites, the manganese ions the octahedral 16d sites, and the oxide ions the 32e sites; the 8b, 48f, and 16c sites remain empty. As for $LiNiO_2$, $LiMn_2O_4$ appears to be difficult to synthesize with this stoichiometry. Furthermore, the structure seems to be unstable during extraction and insertion of lithium. In order to stabilize this spinel material extra lithium is added in the synthesis process, leading to a composition $Li_{1+d}Mn_{2-d}O_4$ where the extra Li^+ ions replace the 16d Mn ions. However, 16c sites are occupied up to 3.5 *m/o* Li [20]. The defect chemistry is different for Li ions on 16c and 16d sites, particularly as the 16c sites are part of the Li-diffusion pathway. Excess Li^+ has a dramatic influence on the capacity of the compound as the overall Mn-oxidation state increases rapidly with increasing excess Li^+. Cation mixing as is observed for $LiNiO_2$ has not been found for this spinel. However, several other spinel-like materials have been reported with for instance oxygen ion vacancies [6,7].

2.2.1. Oxygen deficient spinels; $LiMn_2O_{4-b}$

A number of papers deal with oxygen-deficient spinel materials. Sugiyama et al. [7] proposed three defect models to explain the oxygen-partial pressure dependency of the spinel material, i.e., a point defect model, a simple cluster model, where two Mn(III) ions are bound to an oxygen vacancy, and a complex cluster model, where four Mn(III) ions are bound to two oxygen vacancies. The last model seems to explain their results at best. However, this defect cluster structure will retard Li^+ ion diffusion in the structure.

2.2.2. Extracted forms of $Li_{1-x}Mn_2O_4$

In the case of Li^+ extraction, vacancies on 8a sites in the lithium-ion sublattice are formed. The potential curve as a function of x reveals three regimes [17,21], i.e., between $x = 0$ and $x = 0.4$ a single-phase system, between 0.4 and about 0.75 a two-phase mixture of coexisting spinel phases with different lattice parameters and Li-contents $Li_{0.25}Mn_2O_4$ and $Li_{0.6}Mn_2O_4$, respectively, and below 0.25 a single-phase mixture where Li^+ ions can be extracted only at potentials much higher than 4 V, as they reside probably on octahedral 16c or 16d sites.

3. Magnetic measurements

3.1. Experimental

Powders were synthesized using $LiOH \cdot H_2O$ and $Mn(CH_3COO)_2 \cdot 4H_2O$ in appropriate ratios. The product composition was analyzed by X-ray diffraction, Infra Red spectroscopy and redox titrations. Magnetic susceptibility measurements (Gouy method) were performed in a temperature range of 20 to 250°C using an ordinary magnet (0–3000 G) equipped with a heating chamber and an electronic microbalance. ESR spectra were recorded using a Varian EPR-4 spectrometer.

3.2. Results and discussion

Data of the number of unpaired electrons were derived from magnetic susceptibility measurements [22] using the

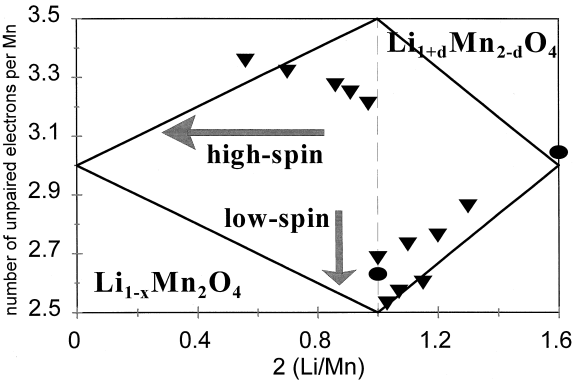

Fig. 1. Number of unpaired electrons of both $Li_{1-x}Mn_2O_4$ (below $2(Li/Mn) = 1$) and $Li_{1+d}Mn_{2-d}O_4$ (above $2(Li/Mn) = 1$) derived from magnetic susceptibility measurements. Theoretical high- and low-spin situations are drawn for comparison. The closed circles (●) are from Blasse [23,25].

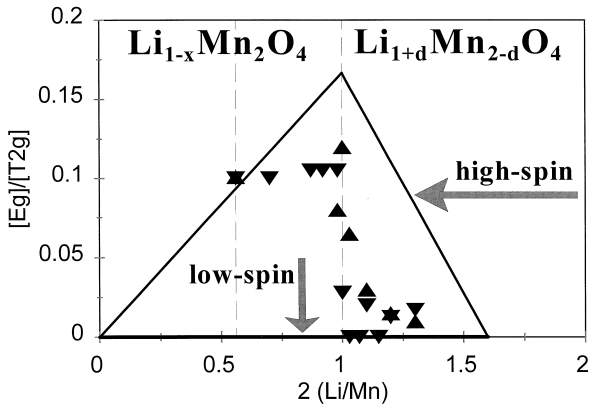

Fig. 3. Distribution ratio of the e_g and t_{2g} orbitals recalculated from Fig. 1 (▼). The figure includes also the ratio of the peak intensities calculated from deconvolution of the ESR spectra of Fig. 2 (▲). The ratio is scaled to $2(Li/Mn) = 0.56$ ($x = 0.44$) of the magnetic susceptibility measurements.

Curie–Weiss law: $1/X_m = c_e/(T - \Theta_c)$ with X_m the molar magnetic susceptibility, c_e the Curie-constant, T the absolute temperature, and Θ_c the Curie-temperature. The results are plotted in Fig. 1. Note that below $2(Li/Mn) = 1$ the values refer to the extracted form, whereas above $2(Li/Mn) = 1$ values refer to $Li_{1+d}Mn_{2-d}O_4$ materials. Theoretical lines are given for the case that the Mn(III)-ions are high- or low-spin. The number of unpaired electrons in $LiMn_2O_4$ agrees quite well with reported data of Blasse [23] and Schütte et al. [24]. ESR measurements are plotted in Fig. 2. The spectra reveal two signals, a small one and a broad one, which are attributed to the e_g and t_{2g} orbitals, respectively. In Fig. 3, the results of the magnetic susceptibility are plotted in a different way, i.e., the ratios of the occupancy of the e_g and t_{2g} orbitals are shown. The peak intensity of the ESR signals derived by deconvolution of the spectra was used as a measure for the occupancy for both orbitals. The results are plotted in Fig. 3 and were scaled to the magnetic susceptibility measurements. A clear agreement was found, hence it seems that the ratio of the occupancy of the e_g and t_{2g} is constant upon extracting lithium. However, as soon as the maximum high-spin situation is reached, the structure is not stable anymore and will precipitate into the two described spinel phases, i.e., $Li_{0.25}Mn_2O_4$ and $Li_{0.6}Mn_2O_4$. A similar precipitation occurs at $x = 1$ if additional lithium is inserted; two coexisting phases appear, i.e., $LiMn_2O_4$ and $Li_2Mn_2O_4$, with the latter showing a tetragonal distortion of the former. However, it must be stressed that there exist two distinct phases having their own number of unpaired electrons. Hence, a sudden transition may expected in the compound itself, but not immediately in a mixture of both as occurs upon insertion.

The $Li_{1+d}Mn_{2-d}O_4$ compounds contain Mn(III) ions only in the low-spin state. The Curie-temperatures Θ_c derived form the measurements are given in Fig. 4. It is stressed that measurements were performed only on extracted spinels having x-values below 0.4, as higher x-values would lead to a phase mixture with undefined parameters. However, above $x = 0.75$ again a single-phase system occurs with enables analyzing this regime too. According to Goodenough [26] and Kanamori [27], the Curie-temperature is a measure of the strength of the magnetic interaction (the 90° exchange interaction) of the $3d^3$-ion octahe-

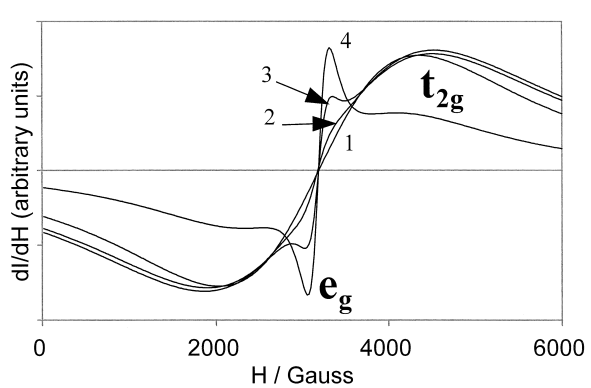

Fig. 2. ESR spectra of both $Li_{1-x}Mn_2O_4$, $x = 0.44$ (1) and $x = 0.02$ (2) and $Li_{1+d}Mn_{2-d}O_4$, $d = 0.0$ (3) and $d = 0.154$ (4).

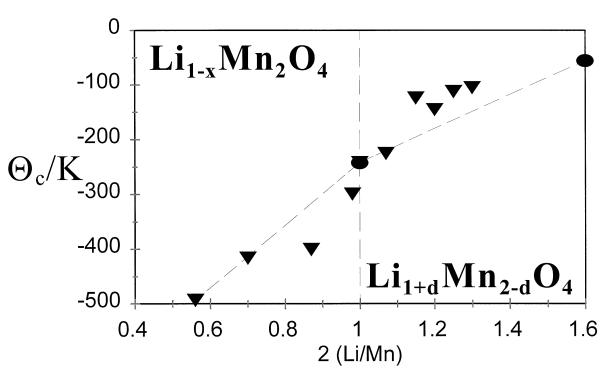

Fig. 4. Curie-temperature Θ_c of both $Li_{1-x}Mn_2O_4$ (below $2(Li/Mn) = 1$) and $Li_{1+d}Mn_{2-d}O_4$ (above $2(Li/Mn) = 1$) derived from magnetic susceptibility measurements. The closed circles (●) are from Blasse [23,25].

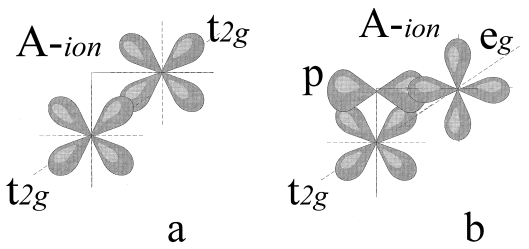

Fig. 5. Orbital overlap describing 90° d^3 interaction: cation–cation interaction causing a strong negative Θ_c (a), cation–anion–cation interaction causing a small negative or even positive Θ_c [25–27].

dral sublattice (see Fig. 5). The overlap of the t_{2g} orbitals determines the strength of the cation–cation interaction, and, therefore, cation and anion sizes are important parameters. A strong interaction gives a strong negative Θ_c. The covalent character, i.e., the overlap of the cation and anion orbitals, determines the strength of the cation–anion–cation interaction. If cation–anion–cation interactions are predominantly small, negative or even positive Θ_c values are found. Consequently, the Θ_c of these materials can provide information on the ionic distribution of the octahedral sublattice of which lithium ions take part, either in $Li_{1-x}Mn_2O_4$ or $Li_{1+d}Mn_{2-d}O_4$.

Increasing x in $Li_{1-x}Mn_2O_4$ reduces the lattice parameter, and consequently an increased overlap of the t_{2g} orbitals can be expected, and, thus, a stronger negative Θ_c, which is indeed observed. Again it is stressed that this holds only for $0 < x < 0.4$.

For $Li_{1+d}Mn_{2-d}O_4$, the lithium ions will break up the interactions due to lack of sufficient orbital overlap, leading to a more positive Θ_c (less negative). This is also clearly observed. At present it is still not clear how the ratio of the e_g and t_{2g} orbitals occupancy is related to the above mentioned interactions. A preliminary explanation may be that a low-spin situation, i.e., only a small fraction of electrons in the e_g orbitals, provides the possibility for an increased covalent character. Thus, accurate measurements of the Curie-temperature and Curie-constant could be helpful in analyzing cluster models such as suggested by Sugiyama et al. [7].

4. Conclusions

It is apparent from the current literature, that the cathode materials, discussed here, exhibit both deviations from molecularity and stoichiometry. These deviations may have an adverse effect on the stability and electrochemical behaviour. The defect chemical notation employed here reveals both the charge and site balance, which is especially important in describing the defect chemistry of doped materials which are being studied to stabilize the structure. Furthermore, magnetic measurements were applied for understanding the electronic structure, which will on its turn reflect in a way the ionic defect chemistry.

Acknowledgements

The authors thank Mrs. H. Huang MSc, Prof. L. Chen, Dr. Ir. A.A. van Zomeren, Ir. F.G.J. Ooms for contributions. One of the authors (JS) is grateful to Prof. H. Tuller for kind hospitality during a sabbatical leave. The technology foundation (STW) and the Netherlands Organization for Scientific Research (NWO) are acknowledged for financial support.

References

[1] O. Yamamoto, Z. Ogumi, M. Moira (Eds.), Proceedings of the Eighth International Meeting on Lithium Batteries, Nagoya, Japan, June 16–21, 1996, Elsevier, 1997.
[2] T. Nagaura, K. Tozawa, Prog. Batteries Solar Cells 9 (1990) 209.
[3] J.R. Dahn, U. von Sacken, M.W. Juzkow, H. Al-Janaby, J. Electrochem. Soc. 138 (1991) 2207.
[4] J.M. Tarascon, D. Guyomard, J. Electrochem. Soc. 138 (1991) 2864.
[5] M.M. Thackeray, M.F. Mansuetto, J.B. Bates, J. Power Sources 68 (1997) 153.
[6] J. Sugiyama, T. Atsumi, T. Hioki, S. Noda, N. Kamegashira, J. Alloys Compounds 235 (1996) 163.
[7] J. Sugiyama, T. Atsumi, T. Hioki, S. Noda, N. Kamegashira, J. Power Sources 68 (1997) 641.
[8] C. Delmas, J.P. Peres, A. Rougier, A. Demourgues, F. Weill, A. Chadwick, M. Broussely, F. Perton, Ph. Biensan, P. Willmann, J. Power Sources 68 (1997) 120.
[9] H. Arai, S. Okada, Y. Sakurai, J.-I. Yamaki, Solid State Ionics 109 (1998) 295.
[10] T.A. Hewston, B.L. Chamberland, J. Phys. Chem. Solids 48 (1987) 97.
[11] Z. Lu, X. Huang, H. Huang, L. Chen, J. Schoonman, Solid State Ionics 109 (1998) in press.
[12] R. Kanno, H. Kubo, Y. Kawamoto, T. Kamiyama, F. Imumi, Y. Takeda, M. Takano, J. Solid State Chem. 110 (1994) 216.
[13] T. Ohzuku, T. Yanagawa, M. Kouguchi, A. Ueda, J. Power Sources 68 (1997) 131.
[14] K. Kube, M. Fujiwara, S. Yamada, S. Arai, M. Kanda, J. Power Sources 68 (1997) 553.
[15] H. Berg, Ö. Bergström, T. Gustafsson, E.M. Kelder, J.O. Thomas, J. Power Sources 68 (1997) 24.
[16] M.M. Thackeray, A. de Kock, M.H. Rossouw, D. Liles, R. Bittihn, D. Hage, J. Electrochem. Soc. 139 (1992) 363.
[17] E.M. Kelder, J. Schoonman, H. Berg, J.O. Thomas, Proc. Electrochem. Soc. 96 (14) (1996) 109.
[18] Y. Gao, J.R. Dahn, J. Electrochem. Soc. 143 (1996) 1783.
[19] F. LeCras, P. Strobel, M. Anne, J.-B. Soupart, J.-C. Rousche, Eur. J. Solid State Inorg. Chem. 33 (1996) 67.
[20] M. Wohlfart, Sixth UECT Electrochemical Symposium Ulm, June 29–30, 1998, Ulm, Germany.
[21] R.J. Gummow, A. de Kock, M.M. Thackeray, Solid State Ionics 69 (1994) 59.
[22] A.A. van Zomeren, E.M. Kelder, J. Schoonman, E.R.H. van Eck, The 1997 Joint International Meeting of the Electrochemical Society and the International Society of Electrochemistry, Meeting Abstract, Vol. 97-2, p. 2507.
[23] G. Blasse, Philips Res. Rep. 3 (1964) Suppl.
[24] L. Schütte, G. Colsmann, B. Reuter, J. Solid State Chem. 27 (1979) 227.
[25] G. Blasse, Philips Res. Rep. 18 (1963) 400.
[26] J.B. Goodenough, Phys. Rev. 117 (1960) 1442.
[27] J. Kanamori, Phys. Chem. Solids 10 (1959) 87.